Superresolution in left-handed composite structures: From homogenization to a detailed electrodynamic description

Vladimir N. Kissel and Andrey N. Lagar'kov
Institute for Theoretical and Applied Electromagnetics, Moscow, 125412 Izhorskaya 13/19, Russia
(Received 7 April 2005; revised manuscript received 20 May 2005; published 8 August 2005)

Experimental results which have demonstrated the effect of superresolution predicted previously by Pendry are dealt with. The "superlens" is provided by a plate of a composite material filled with resonant elements such as spirals with a small pitch and linear half-wave segments of copper wire, excited by the magnetic and electric components, respectively, of a field generated by two linear wire radiators. Integral equations following from Maxwell's equations are applied and solved numerically for a detailed study of the interaction between the electromagnetic wave and the composite material. This solution of the problem in a rigorous formulation enables one to reproduce all details of the electromagnetic processes occurring in the experimental setup while taking into complete account the interaction between all wire resonators making up the experimental plate. A physical interpretation is suggested of the development of an image with superresolution in a real device. The obtained data are compared with the results of a solution of a similar problem in the universally accepted approximation based on the use of averaged constitutive parameters of Maxwell's equations: namely, on the introduction of permittivity and permeability with negative values. The experimental conditions are discussed which are most favorable for the realization of superresolution.

DOI: 10.1103/PhysRevB.72.085111 PACS number(s): 73.20.Mf, 41.20.Jb, 78.20.Ci, 42.30.−d

I. INTRODUCTION

Considerable interest has been shown during the last decade in composite materials of unusual radiophysical and optical properties, the so-called metamaterials. This wide range of artificial dielectrics and magnetodielectrics is not yet clearly defined. Many of the researchers apply the term "metamaterials" to composites which contain inclusions of certain resonance properties and characteristic sizes of less than the wavelength, such as highly conducting needles, split rings, spirals, Ω inclusions, and so on. Also classed with metamaterials in some cases are photon crystals which are ordered composite structures characterized by the dependence of the wave vector k on frequency ω, which is typical of periodic structures.

One of the objectives of theoretical description of metamaterials is to determine their effective parameters—namely, permittivity ε, permeability μ, and the chirality factor—using the results of studies of the properties of individual inclusions (conductivity, permittivity, permeability, and shape), as well as their concentration. Even the well-known monograph by Schelkunoff and Friis[1] gives expressions which describe an artificial magnetic of positive or negative permeability arising owing to the introduction into the composite of capacitance-loaded split rings. Numerous papers published later were devoted to the study of the effective parameters of composites containing needles (see, for example, Ref. 2 and references cited there), rings and spirals,[3,4] Ω inclusions,[5] and so on.

The use of effective parameters in electrodynamic equations for a continuous medium when studying the electromagnetic wave propagation in metamaterials with effective negative permittivity and permeability [so-called left-handed media (LHM)] made it possible to predict a number of surprising effects and suggest a number of interesting devices characterized by special properties (for example, an axisymmetric focusing element involving a cylinder with a coating of metamaterial,[6] elements of microwave-frequency circuits,[7] leaky-wave antennas,[8,9] electronically controlled transmission-line structures,[9] and so on). However, in our opinion, one of the most spectacular of these effects is that of "superresolution" of a focusing system based on the plane-parallel Veselago lens[10] with $\varepsilon=\mu=-1$, which was predicted by Pendry in Ref. 11 and confirmed experimentally.[12,13]

II. SUPERRESOLUTION IN A SYSTEM WITH A THIN HOMOGENEOUS LHM PLATE

Inferences with quantitative estimates of the critical impact of losses on the possibility of realizing the "superresolution" were made almost simultaneously by several teams of researchers.[13–16] However, an important detail was observed and utilized in Refs. 13 and 14; namely, theoretical analysis revealed that the use of *thin* LHM plates brings about a drastic *reduction of loss requirements* and leads one to hope for the possibility of practical utilization of the effect of near-perfect resolution. It was owing to this inference that the requirements of the experimental setup could be formulated and the effect of "superresolution" could be registered under laboratory conditions.[12,13]

We used various methods to check the inferences concerning the physical meaning and quality of image focusing of a point source by a plate of a homogeneous metamaterial (in what follows, we will refer to such media for simplicity as metasubstance). In particular, in addition to a rigorous analytical solution of the boundary problem for an infinite plate, the excitation of a plate of *finite width* by two parallel filaments of cophased electric current was treated. The parameters ε and μ of the material (possibly, anisotropic) were included in the expressions of polarization currents in the plate volume. Then, a set of volume integral equations was composed relative to field components in dielectric using the Green function of free space. Given below is an example of a set of volume integral equations for solving a two-dimensional (2D) diffraction problem, set up with respect to the field components in the dielectric volume V for the case of $\mathbf{E}$ polarization in which the vector $\vec{E}$ of incident fields $\vec{E}^i$ and $\vec{H}^i$ has only one z component and is parallel to the generatrix of an isotropic dielectric cylinder with an arbitrary (in this case, rectangular) shape of the cross section,

$$\begin{pmatrix} \hat{E}_z \\ \mu H_x \\ \mu H_y \end{pmatrix} + \begin{pmatrix} -k^2 & -ik\,\partial/\partial y & ik\,\partial/\partial x \\ -ik\,\partial/\partial y & \partial^2/\partial y^2 & -\partial^2/\partial x\,\partial y \\ ik\,\partial/\partial x & -\partial^2/\partial x\,\partial y & \partial^2/\partial x^2 \end{pmatrix} \begin{pmatrix} \mathbf{L}_\varepsilon \hat{E}_z \\ \mathbf{L}_\mu H_x \\ \mathbf{L}_\mu H_y \end{pmatrix} = \begin{pmatrix} \hat{E}_z^i \\ H_x^i \\ H_y^i \end{pmatrix}.$$

Here, $\hat{E}=E/W$, W is the intrinsic impedance of free space, k is the wave number of free space, $\mathbf{L}_\varepsilon\Psi=\int_V(\varepsilon-1)\Psi G\,dV$, $\mathbf{L}_\mu\Psi=\int_V(\mu-1)\Psi G\,dV$, $G=\exp(-ikr)/4\pi r$ is the Green function of free space, r is the distance between observation and integration points, and $\vec{E}^i$ and $\vec{H}^i$ are the fields of filamentary sources in free space.

The solution of this set of equations gives the components of the total field in the plate volume V. The scattered field at an arbitrary point in space may be readily determined as well if one uses the vector potential theory. For example, the following expression is derived for the z component of scattered field $\vec{E}^s$:

$$\hat{E}_z^s(p) = k^2\int_V(\varepsilon-1)\hat{E}_z G\,dV - ik\frac{\partial}{\partial x}\int_V(\mu-1)H_y G\,dV + ik\frac{\partial}{\partial y}\int_V(\mu-1)H_x G\,dV.$$

As a result, the basic inferences were confirmed without involving the concepts of the double-negative-medium wave number and exponentially decaying or rising wave modes. In addition, the need to choose the desired sheet of Riemann surfaces was obviated. Finally, a model of a finite-width plate is more realistic.

The results of numerical modeling for a plate with a relatively large thickness of the order of half the wavelength at $\varepsilon=\mu=-1-i0.01$ confirmed the absence of superresolution. Zones of local concentration of electromagnetic field energy arise within the plane-parallel plate and in the vicinity of this plate in the neighborhood of the points of crossing of refracted rays, and the direction of energy transport by and large corresponds to the ray representations. However, the size of these "spots" and the achieved resolution (the extremely small distance between the sources, at which their images are discernible separately) showed no advantages over conventional focusing systems.

Much better performance is exhibited by a system based on a thin LHM plate. In particular, even in the case of relatively high losses in the left-handed material, when $\varepsilon''=\mu''=0.1$, one can obtain a sharp separable image of sources separated by a distance of one-tenth a wavelength.

Note that both the calculations and experiments with a thin plate of *finite* width revealed that there is no need to use a large plate for subwavelength imaging of sources. For example, if the plate thickness is about $\lambda/30$ and the sources are spaced at a distance of $\lambda/6$ from one another, their sharp separate images are obtained even for a plate width of $\lambda/4$ to $\lambda/3$; further increase in the plate width does not result in a marked improvement of the quality of image (resolution). This characteristic property of a thin plane-parallel lens appears to be of special interest, because conventional focusing devices must have lenses or mirrors whose sizes exceed significantly the wavelength.

III. DETAILED ELECTROMAGNETIC MODELING

Note, however, that the use of effective parameters to describe rather complex systems such as materials with negative ε and μ is hardly self-evident (though it is efficient) as a tool for studying the wave propagation in metamaterials. For example, it was shown in Ref. 17 that, in the case of composites containing extended resonant inclusions, the effective permittivity may be introduced only for sheet materials whose thickness exceeds some critical value and, generally speaking, the value of permittivity may differ depending on the experimental conditions (see also the discussion in Ref. 18). The experimental determination of the effective parameters of composites containing resonant inclusions is based, as a rule, on the results of measurements under incidence of a wave with a quasiplane front.[19]

We will demonstrate some characteristic features of electromagnetic wave propagation in a real composite and expose the aspects which turn out to be hidden when the effective parameters are used in Maxwell equations. This could be done by applying a rigorous approach (integral equation method) to obtain a full-wave solution for the electromagnetic fields.

A. Experiment

By way of example, we will give the results of a computational experiment which repeats the conditions of real experimental investigations.[13] This latter study involved the use of a plate of a composite with inclusions of resonant elements in the form of spirals with a small pitch and half-wave rods, excited by the magnetic and electric components, respectively, of a field radiated by two linear radiators. The experimental setup is shown schematically in Fig. 1. The microwave image of the sources (half-wave radiators 1 and 2 spaced from each other at a distance that is much less than the wavelength) was recorded by the receiving probe antenna 3 in the process of its displacement parallel to the plate surface, as shown in the figure. The results of field measurements in the absence of a plate between the antennas, as well as when the plate is introduced, are given in Figs. 2(a) and 2(b), respectively. In the latter case, the frequency range (1.65–1.8 GHz) is clearly registered in which a separate im-

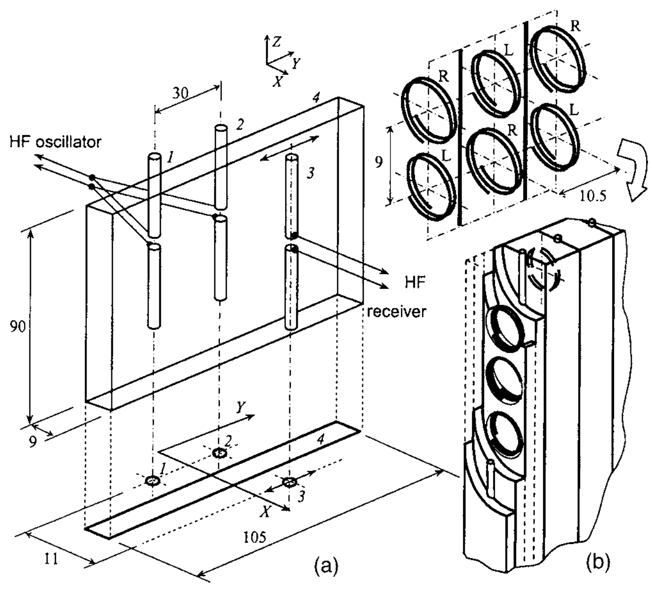

FIG. 1. Schematic of the experimental facility.

age of two closely spaced sources (separated by the distance of only $\lambda/6$) is observed.

Additionally, it was verified that a manufactured plate exhibits some properties typical of a plate of metasubstance, in particular with respect to the negative phase velocity of the wave in such a medium. To confirm this, a plate, first of quartz glass and then of LHM composite, was introduced into the spacing between the field source and receiving antenna. The phase advance $\Delta\varphi$ of the received signal was registered in the process of plate travel (Fig. 3). The emergence of a plate of "standard" material (quartz) between the source and receiving antenna resulted in a positive phase increment. The presence of the LHM plate caused a decrease in the phase advance, which confirms the realization of negative effective ε' and μ' and the emergence of a backward wave in the structure.

Therefore, theoretical predictions of the possibility of overcoming the "diffraction limit" in systems with double-negative materials were used to develop some passive device

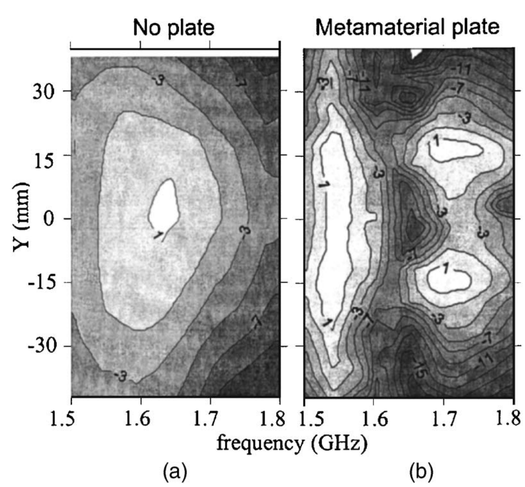

FIG. 2. Microwave images of the filamentary sources in the (a) absence and (b) presence of the metamaterial plate.

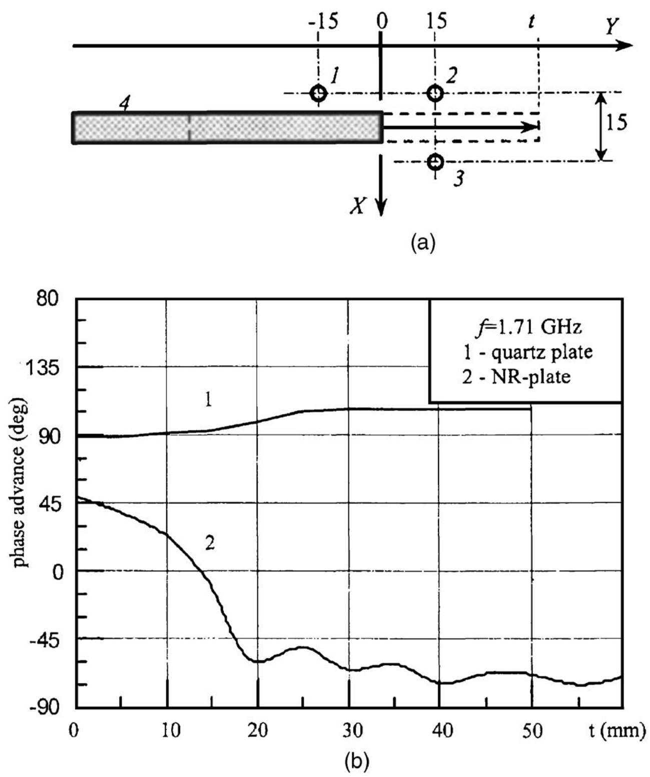

FIG. 3. Phase advance measured in the process of plate displacing between antennas.

which indeed helped to obtain the expected superresolution. However, it would be rather doubtful to identify the electromagnetic processes occurring in an experimental composite plate with electromagnetic-wave transmission through a layer of homogeneous (ideal) metasubstance with $\varepsilon < 0$ and $\mu < 0$. One of the obvious reasons for this is the discrete structure of the composite. It is known[15] that, in regular structures, the value of the lattice spacing constrains the limiting resolution of the system. In this case, however, one more fact is worthy of note. According to Ref. 13, one can count on the manifestation of the effect of superresolution only when thin plates with low loss are employed; therefore, in the setup described above, the plate consisted of only one layer of resonators (see Fig. 1). It is hard to set up a correspondence between this structure and a plate of homogeneous material, even if because of the absence of clearly defined boundaries of the composite in the transverse direction. One can assume that the location of these (conventional) boundaries must depend on the characteristic features of distribution of the electromagnetic field in the vicinity of inclusions. Then, one must not rule out the possibility that the electromagnetic process in a thin-layer composite plate differs significantly from phenomena occurring in a homogeneous material; as a result, the use of the effective parameters of the medium ε and μ will turn out to be incorrect. In any case, the conventional approach based on the ray concepts appears to be clearly inadequate when treating the interaction between the field of a point source and a thin composite plate consisting of a single layer of resonators.

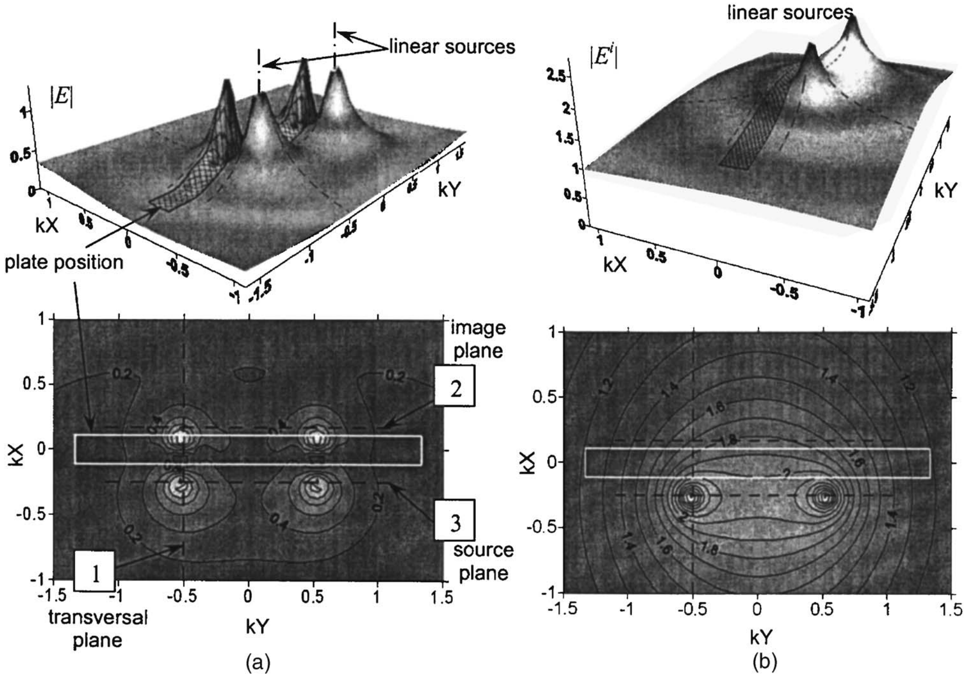

FIG. 4. (a) Fields and characteristic cross sections of their relief when focusing two point sources by a plate of metamaterial and (b) fields in free space.

B. Computational model

In order to construct the computational model, an equation of the Pocklington type was used, which is based on a thin-wire approximation with regard for the finite conductivity of the wire metal including the skin effect by means of introducing specific impedance of the wire material Z,

$$ZI + i\omega\mu_0\int_L I\left(\vec{v}\cdot\vec{v}' - \frac{1}{k_0^2}\frac{\partial^2}{\partial v\ \partial v'}\right)\frac{e^{-ikr}}{4\pi r}dl = \vec{v}\cdot\vec{E}^i,$$

$$L = \sum L_i, \quad Z = \frac{1+i}{2\pi a\sigma d}.$$

This equation is set up relative to the linear current density I in wire elements L_i of a composite; here, $\vec{v}$ and $\vec{v}'$ are unit vectors of tangents to the wire axis at observation and integration points, respectively, r is the distance between these points, and $\vec{E}^i$ is the vector of intensity of incident field of frequency ω. The finite conductivity of the wire metal including the skin effect was also taken into account by introducing its specific (per unit length) impedance Z (d is the skin depth, and a and σ denote the wire radius and conductivity of its material, respectively).

Note that this equation, in the form given above, may be employed directly for the simulation of a composite consisting of spirals and linear conductors. However, in view of the selected geometric parameters or spiral resonators (namely, small spacing between turns, which leads to a significant interturn capacitance), it proves to be more reasonable to turn to a resonator model in the form of a wire ring with a capacitive load connected into a narrow split in the conductor; this approach provides for significant savings in computational resources. In our study, the capacitive load of elements was taken into account through their equivalent (lumped) impedance.

The numerical algorithm of solution of this integral equation was developed using the widely employed Galerkin method (i.e., the moment method with roof top expansion and weighting functions). The scattered field was calculated by the obtained currents using vector potentials.

The thus developed algorithm was thoroughly tested. The wire elements were provided by linear conductors (vibrators) of different length, as well as loops of different shape. All results of the calculation of currents and scattered fields fitted the expected results and the results known from the literature. Described below by way of example is one of the tests for a scatterer in the form of a loaded loop, which gives a qualitative estimate of the accuracy of the results.

Let a circular wire loop of radius $kr = 0.2$ be preassigned with wire radius $ka = 1.466\times 10^{-3}$. The inductance of such loop is described by the approximate reference formula

$$L \approx 4\pi r\left(\ln\frac{r}{a} + 0.079\right)\times 10^{-7}\ \text{Hn}.$$

The inductive impedance of such loop will be $H_L = \omega L \approx 371\ \Omega$. For obtaining resonance, the load must have an inductive impedance of $X_C = -X_L$. The calculation results demonstrated that the resonance in the circuit occurs at $X_C = -377\ \Omega$ (a series of calculations were performed for close values of the load impedance, and the current amplitude was monitored; the circular loop was approximated by an octagon).

In subsequent calculations, the lumped load was replaced by an equivalent segment of a two-wire line (the distance between the conductor axes was $kD = 0.1$; the conductor radius remained the same, $ka = 1.466\times 10^{-3}$). A series of successive calculations revealed that the resonance is observed if the length of the line segment connected instead of the reactive load is $kl = 0.924$. The intrinsic impedance of the employed line may be determined by the reference formula

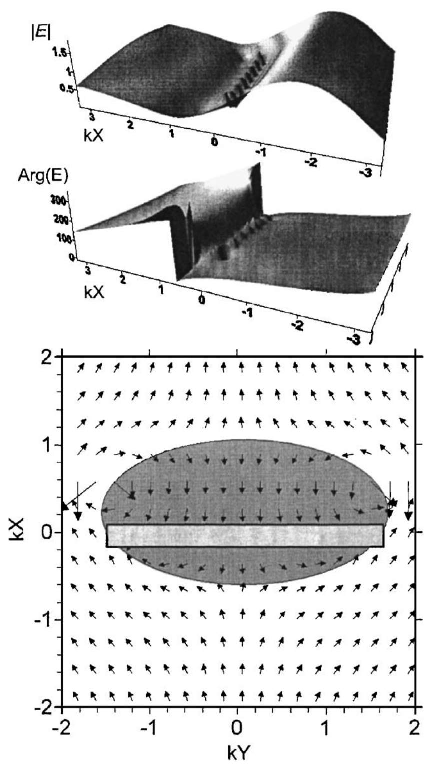

FIG. 5. Magnitude, phase, and phase velocity vectors of the field in the vicinity of the composite LHM plate under plane-wave excitation.

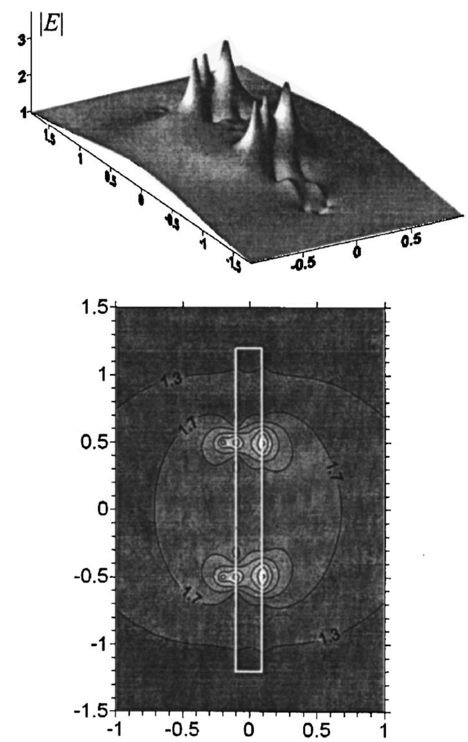

FIG. 6. A field in the vicinity of a metasubstance plate which is excited by two filamentary sources.

$$W = 119.9 \ln(t + \sqrt{t^2 - 1}), \quad \text{where } t = D/2a.$$

In this case, it was $W = 506.2\ \Omega$. In view of this, the equivalent capacitive impedance of the line segment $|X_C| = W\cot(kl)$ turned out to be 382 Ω, which agrees well with the expected value (about 377 Ω). Therefore, the thus developed algorithm correctly takes into account both the electromagnetic interaction between different elements of the conductor and the impact of lumped load.

Note further that numerical investigations were performed both for a finite system of loaded rings and vertical conductors and for an infinite array of similar scatterers (in the latter case, the periodic Green function was used instead of the Green function of free space and, in accordance with the array theory, the integral equation was written for one period of the structure). The numerical algorithms were additionally tested for agreement of the results.

Discussed below are the results of numerical simulation obtained for a composite plate with a finite number of elements which corresponds to that of a real experimental sample.[13] The calculation results both reproduced the observed effect of superresolution in the presence of a complex composite medium and made it possible to compare the phenomena occurring in real samples of composites (periodic systems of resonant elements) to phenomena occurring in homogeneous media with negative electrodynamic parameters (metasubstances) which exist only theoretically.

It has been demonstrated that a plate of a composite exhibits some properties typical of a plate of metasubstance. For example, a frequency band exists (as predicted by theory, it is located in the vicinity of and a little higher than the resonance frequency of inclusions) in which the effect of superresolution shows up. It is well seen in Fig. 4(a), in whose top part the surface relief is shown and in the bottom part—the isolines of intensity of an electric field calculated in the plane of the central cross section of the plate and in its neighborhood.

For comparison, Fig. 4(b) gives analogous patterns in the absence of a plate (all geometrical dimensions along the graph axes are given in electrical units—i.e., are multiplied by $k = 2\pi/\lambda$, where λ is the wavelength in free space).

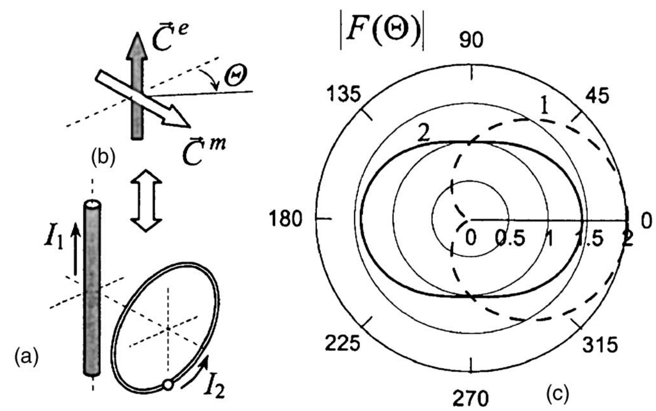

FIG. 7. The equivalent electric and magnetic moments of a system of linear and ring conductors and its far-field patterns realized at different values of relative phase shift of currents in the conductors.

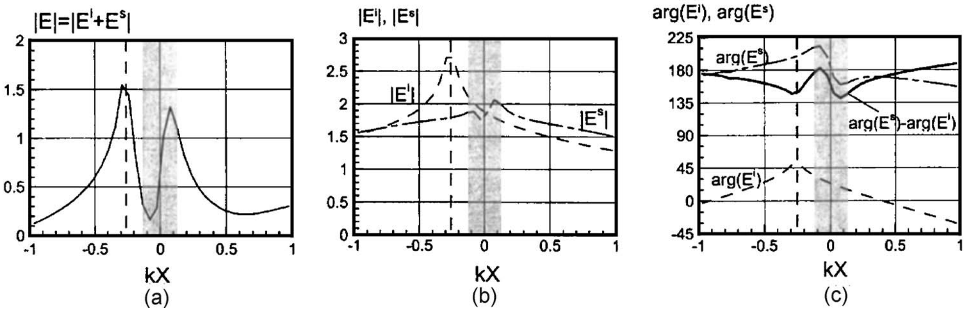

FIG. 8. Components of fields in cross section 1 (see Fig. 4), calculated at frequency $f=1.05f_0$.

The composite plate proper may be by and large characterized as a device in which a backward wave exists; i.e., there is a zone of space in the vicinity of resonators in which the phase and group velocities are opposite to each other. Figure 5 shows (see from the top down) the distributions of the amplitude, phase, and vector of phase velocity of total field (E_z component) in the vicinity of the composite plate, when a plane wave propagating in the direction of the Y axis is incident on this plate.

C. Physical interpretation of near-perfect imaging

However, one can readily see the differences in the field distribution between a thin composite plate and a plate of metasubstance. For example, in a system with a homogeneous plate with $\varepsilon=\mu=-1$, the phase and group velocities bear different signs only within the plate, and a strong excitation of the composite plate bars leads to the emergence of a zone with negative phase velocity outside of the geometric bounds of the structure (see Fig. 5). It is further known (e.g., Refs. 20 and 13; see also Fig. 6) that, when a plane-parallel plate of metasubstance is excited, the reactive energy of evanescent modes accumulates in the vicinity of the interfaces (first of all, in the neighborhood of the unilluminated face of the plate), owing to which the superresolution may be realized. No such interfaces exist in the experimental plate; however, resonance phenomena are present, and the field energy accumulates within and in the vicinity of individual resonators (a maximum of the accumulated reactive energy is attained in the central part of the composite plate in the vicinity of the axial lines of inclusions).

At the same time, one can note that the fields of propagating harmonics and evanescent modes, which make up the spatial spectrum of radiation of the filamentary source, excite the resonators of the composite *differently*. This difference is largely due to the fact that, in the incident field of propagating harmonics (plane waves), the vectors $\vec{E}$ and $\vec{H}$ are in phase, while the evanescent modes are characterized by a phase shift of 90° between the vectors $\vec{E}$ and $\vec{H}$. Further, it is known that the phase and amplitude patterns of a system consisting of crossed magnetic and electric dipoles (models of resonators of composite) are defined by the relation of the phases of currents of these dipoles.

For example, the currents in the elementary cells of the composite—i.e., in resonators I_1 and I_2 [Fig. 7(a)]—define the values of the equivalent electric and magnetic moments C^e and C^m and, in the final analysis, the effective values of ε and μ of the material, Fig. 7(b). Given the appropriate correlation between the absolute values of $|C^e|$ and $|C^m|$ and depending on the phase difference $\Delta\varphi$ between them, far-field patterns may be realized such as, for example, those of form 1 (at $\Delta\varphi=0°$) or of form 2 (at $\Delta\varphi=90°$), Fig. 7(c). Two different cases of excitation of a structure may be readily made to correspond to these patterns: namely, excitation by the field of propagating wave (with zero phase shift $\Delta\varphi$ between the vectors of electric and magnetic fields) or by the field of exponentially evanescent harmonic (when $\Delta\varphi=90°$).

Investigations reveal that the realization of suitable phase relations in the electric and magnetic resonators of the plate results in such an interference of the field of their radiation with the incident wave field that the propagating harmonics (in contrast to the evanescent modes) experience a significant attenuation, and specific subwavelength maxima of field intensity arise in the vicinity of the unilluminated face of the plate. One can use these maxima for registering the location of sources with superresolution, as was done in the experiment.

This is confirmed by the graphs which show the distribution of the E_z component of the amplitudes and phases of the total E, incident E^i, and scattered E^s fields calculated along

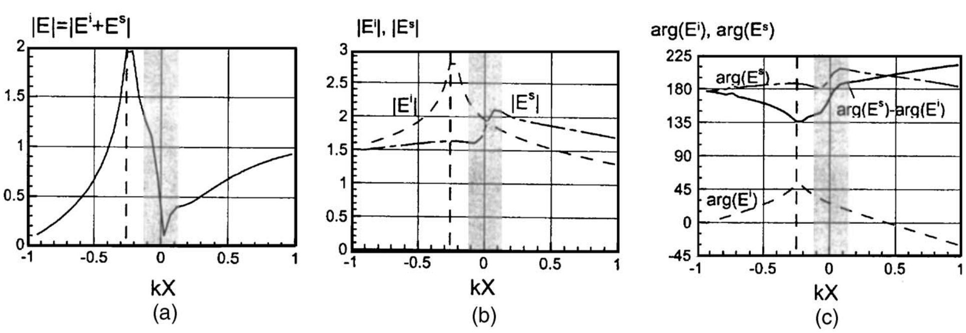

FIG. 9. Components of fields in cross section 1 (see Fig. 4), calculated at frequency $f=0.95f_0$.

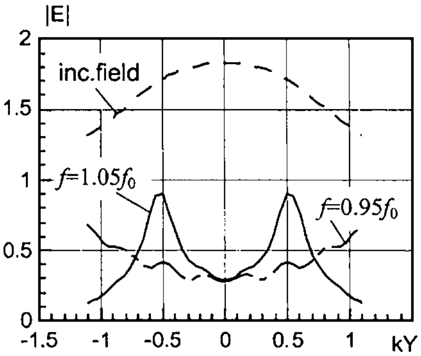

FIG. 10. Fields in cross section 2; see Fig. 4.

the characteristic directions (cross sections) in the space in the vicinity of the plate [Secs. I–III—see Fig. 4(a)].

Let f_0 be the resonance frequency of inclusions of composite. Figures 8 and 9 give the results of calculations on frequencies $f=1.05f_0$ and $f=0.95f_0$ in Sec. I extending normally to the plate through one of the filamentary sources. The source position (in the point of $ky \approx -0.26$) and the region of space $|ky| < 0.11$ taken up by the plate are also shown in these drawings.

One can see that, in the first case [$f=1.05f_0$; see Fig. 8(a)], a field maximum is formed in the vicinity of the rear (with respect to the sources) face of the plate, at $ky \approx 0.1$. This maximum corresponds to one of the peaks of separate images of radiators. The peaks are seen in Fig. 10 which shows the field amplitude in the plane of motion of the measuring probe—i.e., in Sec. II; the dashed line corresponds to the calculation of the incident field—i.e., to the absence of a plate in which the sources are not observed separately.

As to the second case [$f=0.95f_0$; see Figs. 9(a) and 10], no such peaks are formed on a frequency a little below the resonance frequency and no superresolution is observed; the low level of the field in Sec. II is due to the fact that the incident and scattered fields have close amplitudes and are in fact out of phase [see Figs. 9(b) and 9(c)]. Note that the effective ε' and μ' of the homogenized composite (metasubstance) are known to be positive at this frequency.

When tuning from the frequency $f=0.95f_0$ to $f=1.05f_0$, the field amplitudes vary little [compare Figs. 8(b) and 9(b)], unlike the phase relations. As was proved by calculations, it was the excitation of resonators by the evanescent modes that produced the main effect on the phase of the scattered field [compare Figs. 8(c) and 9(c)]. As a result, the superresolution effect emerged.

It is interesting that, when the superresolution is realized (in our case, at $f=1.05f_0$), a characteristic field minimum arises in the vicinity of the "illuminated" boundary; this is again due to interference [see Fig. 8(a), $ky \approx -0.1$]. Therefore, it is to be expected that, as the resonator sizes are reduced and the number of their layers is increased, the layers which are farther away from the illuminated face will be excited more strongly than the front layers; this will result in the known pattern of "rise" of amplitudes of evanescent modes, which is typical of the field in a plate of metasubstance.

Note finally that, when either magnetic or electric resonators are left out of the composite, the superresolution effect will naturally disappear [Figs. 11(a) and 11(b), respectively, $f=1.05f_0$]. Nevertheless, it is confirmed by the calculation results that the resolution may be improved somewhat [see Fig. 11(a)] in extremely thin nonresonance systems of, for example, parallel metal conductors (analogs of thin films with $\varepsilon < 0$).

IV. CONCLUSION

Thus, the main differences in the pictures of field distribution, which are registered in composite materials and in plates of homogeneous metasubstance, are defined by the characteristic features of the employed resonators, in particular by the degree of their electromagnetic coupling with the environment, by the number of layers in the transverse direction of the plate, and (to a lesser extent) by the discrete

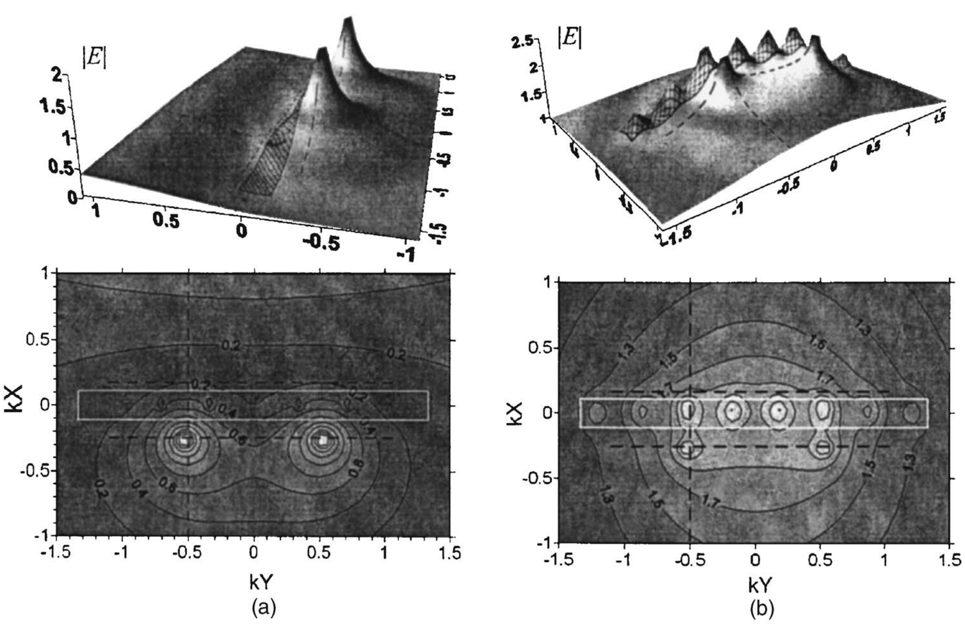

FIG. 11. Fields in the vicinity of a plate of composite consisting of resonators of only (a) electric and (b) magnetic type.

structure of the composite. Because the field of resonators extends significantly beyond the geometric bounds of the sample (including the zone of location of radiators and the zone of measurements), there is no point in using the effective values of the parameters ε and μ in the considered case. Despite the usefulness of the models based on the introducing effective ε and μ, the further improvements in the design of the focusing metamaterial structures are likely to be achieved through using full-wave solution of the electromagnetic boundary problem.

ACKNOWLEDGMENT

The study was supported in part by President Program on Support of Leading Scientific Schools, Grant No. 1694.2003.8.

[1] S. A. Schelkunoff and H. T. Friis, *Antennas: Theory and Practice* (Wiley, New York, 1952).
[2] A. N. Lagarkov and A. K. Sarychev, Phys. Rev. B **53**, 6318 (1992).
[3] A. N. Lagarkov, V. N. Semenenko, V. A. Chistyaev, D. E. Ryabov, S. A. Tretyakov, and C. R. Simovski, Electromagnetics **17**, 213 (1997).
[4] J. B. Pendry, A. J. Holden, D. J. Robbins, and W. J. Stewart, IEEE Trans. Microwave Theory Tech. **47**, 2075 (1999).
[5] M. M. Saadoun and N. Engheta, Microwave Opt. Technol. Lett. **5**, 184 (1992).
[6] A. N. Lagarkov and V. N. Kisel, Phys. Dokl. **46**, 163 (2001).
[7] C. Caloz and T. Itoh, IEEE MTT-S Int. Microwave Symp. Dig. **1**, 195 (2003).
[8] T. Grbic and G. V. Eleftheriades, IEEE AP-S Int. Symp. **4**, 340 (2002).
[9] S. Lim, C. Caloz, and T. Itoh, IEEE Trans. Microwave Theory Tech. **52**, 2678 (2004).
[10] V. G. Veselago, Sov. Phys. Usp. **10**, 509 (1968).
[11] J. B. Pendry, Phys. Rev. Lett. **85**, 3966 (2000).
[12] A. N. Lagarkov and V. N. Kissel, in *Proceedings of the International Conference on Materials for Advanced Applications, Symposium F: Electromagnetic Materials, Singapore, 2003*, edited by L. Hock, O. C. Kim, S. Matitsine, and G. Y. Beng (World Scientific, Singapore, 2003), p. 157.
[13] A. N. Lagarkov and V. N. Kissel, Phys. Rev. Lett. **92**, 077401 (2004).
[14] A. N. Lagarkov and V. N. Kissel, in *Proceedings of the International Conference on Materials for Advanced Applications, Symposium F: Electromagnetic Materials, Singapore, 2003*, edited by L. Hock, O. C. Kim, S. Matitsine, and G. Y. Beng (World Scientific, Singapore, 2003), p. 145.
[15] D. R. Smith, D. Schurig, M. Rosenbluth, S. Schultz, S. A. Ramakrishna, and J. B. Pendry, Appl. Phys. Lett. **82**, 1506 (2003).
[16] X. S. Rao and C. K. Ong, Phys. Rev. E **68**, 067601 (2003).
[17] A. P. Vinogradov, D. P. Makhnovsii, and K. N. Rozanov, J. Commun. Technol. Electron. **44**, 317 (1999).
[18] L. Liu, S. M. Matitsine, Y. B. Gan, and K. N. Rozanov., Electromagnetics **25**, 69 (2005).
[19] D. R. Smith, S. Schultz, P. Markoš, and C. M. Soukoulis, Phys. Rev. B **65**, 195104 (2002).
[20] T. J. Cui, Z.-C. Hao, X. X. Yin, W. Hong, and J. A. Kong, Phys. Lett. A **323**, 484 (2004).